The 2015 World Congress on
Advances in Structural Engineering and Mechanics (ASEM15)
Incheon, Korea, August 25-29, 2015

Dynamic properties of sandwich beam integrating shear thickening fluid under harmonic excitation

*Minghai Wei[1)], Gang Hu[2)], Li Sun[3)], Kun Lin[4)] and Dujian Zou[4)]

[1)] *Department of Engineering Management, Shenyang Jianzhu University, Shenyang 110168, China*
[2)] *Department of Civil and Environmental Engineering, The Hong Kong University of Science and Technology, Hong Kong, China*
[3)] *School of Civil Engineering, Shenyang Jianzhu University, Shenyang 110168, China*
[4)] *Shenzhen Graduate School, Harbin Institute of Technology, Shenzhen 518055, China*
[1)] hitsz.civil@gmail.com

ABSTRACT

The behavior of shear thickening fluid (STF) under impact loadings has received considerable attention due to the field-responsive nature of STF. Few studies have investigated dynamic properties of a structure integrating STF under a harmonic excitation. The harmonic wave is one of the simplest mechanical wave. Other more complex waves, such as a seismic wave, can be considered as a combination of a series of different harmonic waves. In this study, a model of sandwich beam integrating STF under a harmonic excitation was proposed based on theoretical method. The effects of both amplitude and frequency of the harmonic excitation on the natural frequency of the sandwich beam were investigated. Results show that the natural frequency significantly varies with increasing the amplitude or frequency of the excitation. The phenomenon verifies a potential application of the sandwich beam integrating STF to resist the seismic excitation or other periodic excitations.

1. INTRODUCTION

The shear thickening fluid (STF) is endowed with tunable damping and stiffness characteristics by its field-responsive nature (Petel 2013). Compared with the shape memory alloy (SMA) wires (Nehdi 2011, Youssef 2012, Marcelo 2015, Salari 2015) and magneto rheological (MR) fluids (Jiang 2012, Han 2013, Yazid 2014, Hernandez 2015), which modify their own dynamic properties via external stimuli, the response of the STF does not require an external power system. In detail, when the shear rate of STF

[1), 4)] Doctor
[2)] Graduate Student
[3)] Professor

exceeds a critical value, STF exhibits a high-energy absorption behavior and becomes stiff immediately (Waitukaitis 2012). Moreover, processes of the energy absorption and deformation of STF are reversible (Jiang 2013). Due to these properties, STF has been widely used as a resistance material in the impact and explosive field.

Regarding to potential applications of STF in engineering fields, Soutrenon and Michaud (2014) evaluated the efficiency of the STF/foam/silicone composite pads under impact loadings by using a free fall impact tower. The results show that the energy absorption ratio can be up to 85%. Fischer et al.(2006, 2010) investigated the tuning part stiffness and damping capacity of a composite structures with two different STFs under free vibration by using both experimental and finite element analysis methods. Additionally, Zhang et al. (2008) presented a prototype STF damper in flow mode and meanwhile its dynamic properties were experimentally and theoretically studied. Recently, the passive damper filled with STF was developed by Yeh et al.(2014). They found that the area and shape of hysteresis loops in the STF-filled damper vary with changing loading conditions.

To the authors' knowledge, very few studies have been concentrated on dynamic properties of STF under a harmonic excitation. In principle, the harmonic excitation is quite different to an impact load. The former one changes periodically with time, while the latter one is a transient load with a fast changing amplitude and a short duration. In the present study, potential applications of STF in civil engineering, such as applied to reduce seismic responses of civil structures, were studied. The seismic wave is normally considered as a combination of a series of different harmonic waves. Therefore, a sandwich beam integrating STF under a harmonic excitation was investigated theoretically. Meanwhile, effects of both amplitude and frequency of the harmonic excitation on the natural frequency of the sandwich beam were numerically investigated as well.

2. Model formulation

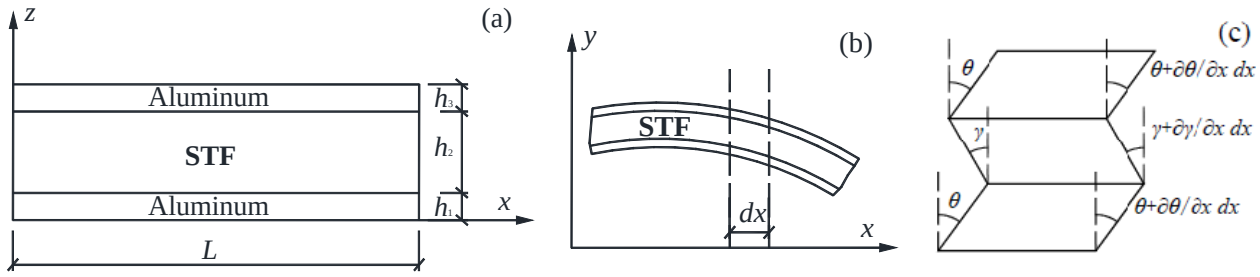

Fig. 1. (a) Sandwich beam with STF core subjected to periodic load; (b) Deformed configurations of sandwich beam; (c) Differential element.

A sandwich beam with a STF core and conductive aluminum skins subjected to a harmonic excitation is shown in Fig. 1. As presented in Fig. 1(a), the beam has a length L and width b. The thicknesses of the bottom, core, and top layers are h_1, h_2, and h_3, respectively. The longitudinal stresses in the mid-planes of the bottom, core, and top layers in the x-direction are σ_1, σ_2, and σ_3, respectively. Some assumptions are made as follows: (a) the deformations of top and bottom layers obey the Euler Bernoulli beam

theory; (b) only the lowest mode of vibration is considered for the beam; (c) the STF core deforms only due to shear; (d) the three layers have the same transverse displacement *z*; (e) there is no slippage and delamination between the adjacent layers during deformation.

Based on the above assumptions, the governing equation of motion for the sandwich beam is obtained by using the complex stiffness method (Ross 1959, Kerwin 1959) as follow

$$B(\frac{\partial^4 v(x,t)}{\partial x^4}) + m(\frac{\partial^2 v(x,t)}{\partial t^2}) = f(x,t) \tag{1}$$

where $f(x, t)$ is the harmonic excitation; $v(x, t)$ is displacement in the z-direction, m is mass per unit length of the beam; B is the complex stiffness. In the present case, the complex stiffness is the dominant dynamic property for energy loss. $v(x, t)$ and $f(x, t)$ are assumed to have the following form

$$v(x,t) = \sum_{n=1}^{\infty} \sin(\frac{n\pi x}{L}) q_n(t) \tag{2}$$

$$f(x,t) = F\exp(i\Omega t)\delta(x - x_0) \tag{3}$$

where F and Ω are the amplitude and frequency of the harmonic excitation, respectively; x_0 is the excitation location; δ is the Dirac delta function.

After substituting Eq. (2) and Eq. (3) into Eq. (1), the governing equation can be rewritten as follows according to the orthogonality condition.

$$\ddot{q}_n(t) + \omega_n^2 q_n(t) = \frac{F}{m}\sin(\frac{n\pi}{L}x_0)\exp(i\Omega t) \tag{4}$$

where $\omega_n^2 = B/m$, which denotes the natural frequency of the n order mode.

The solution of Eq. (4) is

$$q_n(t) = \frac{F}{m}\sin(\frac{n\pi}{L}x_0)\frac{\exp(i\Omega t)}{\omega_n^2 - \Omega^2} \tag{5}$$

Consequently, the transverse displacement in the time domain is expressed as

$$v(x,t) = \sum_{n=1}^{\infty} \sin(\frac{n\pi}{L}x)\frac{F}{m}\sin(\frac{n\pi}{L}x_0)\frac{\exp(i\Omega t)}{\omega_n^2 - \Omega^2} \tag{6}$$

Furthermore, in the frequency domain, it can be expressed as

$$v(x,\Omega) = \sum_{n=1}^{\infty} \sin(\frac{n\pi}{L}x)\frac{F}{m}\frac{\sin(\frac{n\pi}{L}x_0)}{\omega_n^2 - \Omega^2} \tag{7}$$

According to Mead and Markus19, the shear strain in the STF core is

$$\gamma(x,t) = \frac{\delta v(x,t)}{\delta x} + \frac{h_3 + h_1}{2h_2}\frac{\delta v(x,t)}{\delta x} \tag{8}$$

Accordingly, the shear strain rate in the frequency domain has the following form

$$\dot{\gamma}(x,\Omega) = \frac{h_1 + h_3 + 2h_2}{2h_2}\frac{F_0}{m}\frac{n\pi}{L}\cos(\frac{n\pi x}{L})\sin(\frac{n\pi x_0}{L})\frac{1}{\left|\omega_n^2 - \Omega^2\right|} \tag{9}$$

In terms of the above assumptions (c) and (e), a complete transfer of stresses occurs between adjacent layers of the sandwich beam. The complex stiffness can be obtained from the flexural rigidity as

$$M = \int_0^{h_1} \sigma_1 y dy + \int_{h_1}^{h_1+h_2} \sigma_2 y dy + \int_{h_1+h_2}^{h_1+h_2+h_3} \sigma_3 y dy = M_1 + M_2 + M_3 \tag{10}$$

where M_2 = 0; M_1 and M_3 are

$$M_1 = \int_0^{h_1} \sigma_1 y dy = (\frac{E_1 b h_1^3}{12} + E_1 h_1 D^2) \frac{\delta\theta}{\delta x} \tag{11}$$

$$M_3 = \int_{h_1+h_2}^{h_1+h_2+h_3} \sigma_3 y dy = (\frac{E_3 b h_3^3}{12} + E_3 h_3 (\frac{h_1+2h_2+h_3}{2} - D)^2) \frac{\delta\theta}{\delta x} - E_3 h_3 (\frac{h_1+2h_2+h_3}{2} - D) h_2 \frac{\delta\gamma}{\delta x} \tag{12}$$

where D is the z-coordinate of the neutral layer position; θ is defined in Fig. 1(c).

Under certain conditions, which are often met for sandwich beam, the complex stiffness can be approximated as

$$B = (\frac{E_1 b h_1^3}{12} + \frac{E_3 b h_3^3}{12}) + (E_1 h_1 D^2 + E_3 h_3 (\frac{h_1+2h_2+h_3}{2} - D)^2) - E_3 h_3 (\frac{h_1+2h_2+h_3}{2} - D) \frac{\frac{h_1+2h_2+h_3}{2} - D}{1 + \frac{G}{E_3 h_3 p^2}} \tag{13}$$

For the sandwich beam subjected a transverse vibration, the longitudinal force of the cross section is zero as

$$F = \int_0^{h_1} \sigma_1 dy + \int_{h_1}^{h_1+h_2} \sigma_2 dy + \int_{h_1+h_2}^{h_1+h_2+h_3} \sigma_3 dy = 0 \tag{14}$$

where σ_1, σ_2, and σ_3 are

$$\sigma_1 = E_1 y \frac{\delta\theta}{\delta x} \tag{15}$$

$$\sigma_2 = E_2 y \frac{\delta\theta}{\delta x} - E_2 [y - (\frac{h_1}{2} - D)] \frac{\delta\gamma}{\delta x} \tag{16}$$

$$\sigma_3 = E_3 y \frac{\delta\theta}{\delta x} - E_2 h_2 \frac{\delta\gamma}{\delta x} \tag{17}$$

in which, E_1, E_2, and E_3 are the tensile stiffness of unit width for the three layers accordingly.

For the z-coordinate of the neutral layer position D, substituting Eqs. (15)-(17) into Eq. (14) yields

$$D = \frac{E_2 h_2 \frac{h_1+h_2}{2} + E_3 h_3 \frac{h_1+2h_2+h_3}{2} - (\frac{1}{2} E_2 h_2 + E_3 h_3) h_2 \frac{\delta\gamma}{\delta\theta}}{E_1 h_1 + E_2 h_2 + E_3 h_3} \tag{18}$$

For a simply supported beam, the steady motion under a harmonic excitation has a harmonic form. Thus, D can be written as

$$D = \frac{E_2 h_2 \frac{h_1+h_2}{2} + E_3 h_3 \frac{h_1+2h_2+h_3}{2}}{E_1 h_1 + E_3 h_3 + E_3 h_3 \frac{E_1 h_1 \Omega^2}{G}} \tag{19}$$

The dynamic modulus G of STF generally consists of storage modulus G' and loss modulus G'', which are all dependent on the shear rate. The relationship between the three modulus is

$$G = G' + iG'' \tag{20}$$

3. Material

In the present study, STF used was based on fumed silica that has a primary particle size of 14 nm and a surface area of approximately 200 m^2g^{-1} (Zhang 2008, 2008). Based on the study of Zhang et al.(2008, 2008), the viscoelastic behavior of the sample against the dynamic shear rate is plotted in Fig.2. It can be seen that the theoretical moduli based on Eqs. (21)-(22) agree well with the experiment data. Both the loss modulus *G*" and the storage modulus *G*' suddenly increase to a much higher level, which occurs at the range of dynamic shear rate from 100 to 800 s^{-1}.

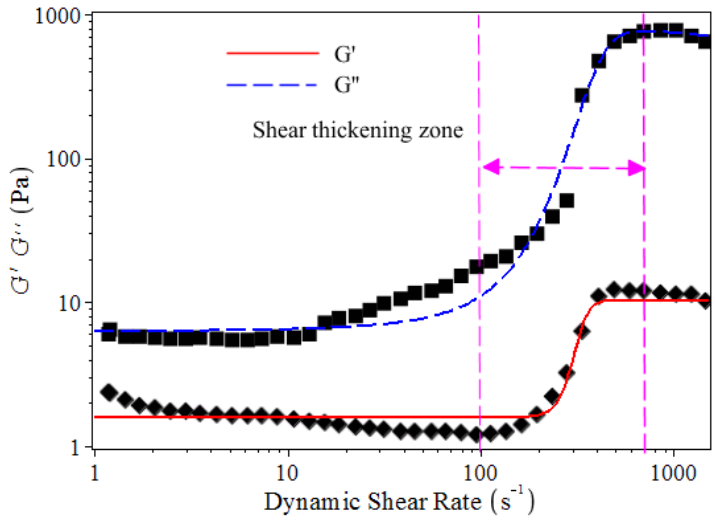

Fig. 2 Apparent modulus function of the storage and loss modulus of the STF compared to the experiment data from the reference (Zhang 2008, 2008).

$$G'(\dot{\gamma}) = 1.573 + \frac{8.755\left(1 - \frac{1}{1+\exp(-0.023\dot{\gamma} + 178.930)}\right)}{1+\exp(-0.038\dot{\gamma} + 12.275)} \tag{21}$$

$$G''(\dot{\gamma}) = 5.211 + \frac{830.151\left(1 - \frac{1}{1+\exp(-0.00092\dot{\gamma} + 3.010)}\right)}{1+\exp(-0.017\dot{\gamma} + 6.606)} \tag{22}$$

After substituting Eqs. (19)-(22) into Eq. (13), it is apparent that the complex stiffness of the sandwich beam is a function of the shear strain rate, as well as a function of the location, amplitude and frequency of harmonic excitation. Furthermore, the stiffness varies along the horizontal direction, i.e. the *x*-direction.

4. Results and Discuss

For the STF-cored sandwich beam as shown in Fig. 1, physical parameters and material properties of the evaluated beam are set to $E_1 = E_3$ =72 GPa, L = 416 mm, b = 30 mm, $h_1 = h_3$ = 1 mm, h_2 = 3 mm, and ρ = 2700 kg/m^3 (Nayak 2014). In order to assess dynamic properties of the sandwich beam, the location of excitation x_0 is set to $L/2$, and the point with x = 0 is selected to be investigated due to the largest shear stain

rate at this point. The natural frequency of the sandwich beam is investigated under different harmonic excitations, for which excitation amplitudes and frequencies are varied.

The natural frequency of the sandwich beam versus the excitation frequency (Ω) under different excitation amplitudes (F) is shown in Fig. 3. As can be seen, when the excitation amplitude is small, i.e. F = 1 N and 10 N, the natural frequency exhibits a significant decrease in the range of $\Omega \leq 4$ rad/s. However, for a large excitation amplitude, i.e. 100 N ≤ F ≤ 5000 N, the reduction in the natural frequency becomes less significant. Furthermore, the reduction ceases at a critical Ω and becomes an increase beyond the critical Ω. The critical Ω is much lower than 4 rad/s and reduces progressively with increasing F. It should be mentioned that the increase in the natural frequency beyond the critical Ω changes to a decrease at a certain Ω, which forms a peak for the natural frequency at this Ω. The peak gradually shifts left with increasing F. Meanwhile, the peak value of the natural frequency is larger than its initial value for $F \geq$ 1000 N, which implies that the stiffness of the sandwich beam becomes larger. The observations indicate that the natural frequency of the sandwich beam integrating STF is dynamic rather than invariant under different harmonic excitations, unlike those of conventional structures. Moreover, the natural frequency becomes more sensitive with increasing the excitation amplitude.

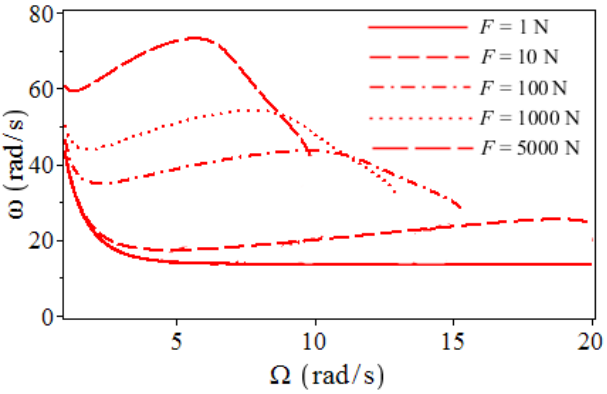

Fig. 3. Natural frequency vs. excitation frequency under different excitation amplitudes.

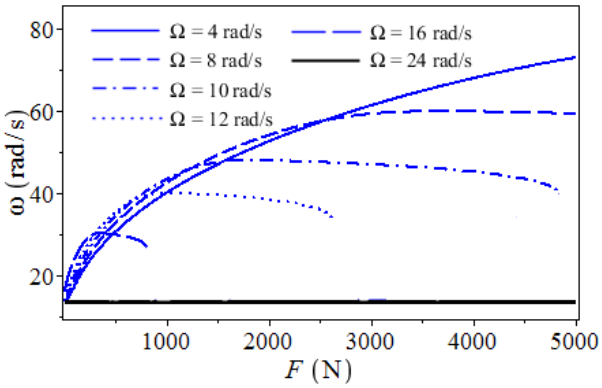

Fig. 4. Natural frequency vs. excitation amplitude under different excitation frequencies.

The natural frequency of the sandwich beam versus the excitation amplitude (F) with a series of excitation frequency (Ω) is shown in Fig. 4. For small excitation frequencies, i.e. Ω = 4 rad/s and 8 rad/s, the natural frequency increases as F is increased. However, for larger excitation frequencies, i.e. Ω = 10 rad/s, 12 rad/s, and 16 rad/s, the natural frequency first increases with F and then decreases beyond a critical value of F. In fact, for Ω = 4 rad/s and 8 rad/s, the natural frequency curves also have a decrease trend beyond a critical value of F; the absence of the decrease trend in Fig. 4 is due to larger critical values than the maximum x-coordinate, i.e. 5000 N, for both cases. The critical values for Ω = 4 rad/s and 8 rad/s are 80000 N and 9750 N respectively. It is apparent that the increase in the natural frequency with F is less significant and more limited with increasing Ω. Compared with the cases with these low

excitation frequencies, a very different phenomenon is observed in the case with a large enough Ω, i.e. $\Omega \geq 24$. The natural frequency remains invariant under various excitation amplitudes in this case, similar to dynamic properties of conventional materials or structures. Based on these observations, it can be concluded that the natural frequency of the sandwich beam integrating STF is more sensitive to the variation of the excitation amplitude in the case with a small excitation frequency compared with a large one.

5. CONCLUSIONS

The present study demonstrates that the natural frequency of a sandwich beam integrating STF varies significantly with both amplitude and frequency of a harmonic excitation. In other words, the natural frequency of the sandwich beam varies with changing the amplitude or frequency of the harmonic excitation. More importantly, the variation is more remarkable with large excitation amplitudes and low excitation frequencies. The findings verify a potential application of the sandwich beam integrating STF to resist the seismic excitation or other periodic excitations.

REFERENCES

Petel, O.E., Ouellet, S., Loiseau, J., Marr, B.J., Frost, D.L., Higgins, A.J., (2013), “The effect of particle strength on the ballistic resistance of shear thickening fluids”. Appl Phys Lett. **102**(6).

Nehdi, M., Alam, M.S., Youssef, M.A., (2011), “Seismic behaviour of repaired superelastic shape memory alloy reinforced concrete beam-column joint”. Smart Struct Syst. **7**(5), 329-348.

Youssef, M., Elfeki, M., (2012), “Seismic performance of concrete frames reinforced with superelastic shape memory alloys”. Smart Struct Syst. **9**(4), 313-333.

Savi, M.A., Pacheco, P.M.C.L., Garcia, M.S., Aguiar, R.A.A., Souza, L.F.G.d., Hora, R.B.d., (2015), “Nonlinear geometric influence on the mechanical behavior of shape memory alloy helical springs”. Smart Mater Struct. **24**(3), 035012.

Salari, N., Asgarian, B., (2015), “Seismic response of steel braced frames equipped with shape memory alloy-based hybrid devices”. Struct Eng Mech. **53**(5), 1031-1049.

Jiang, Z., Christenson, R., (2012), “A fully dynamic magneto-rheological fluid damper model”. Smart Mater Struct. **21**(6), 065002.

Han, Y., Hong, W., Faidley, L.E., (2013), “Field-stiffening effect of magneto-rheological elastomers”. Int J Solids Struct. **50**(14–15), 2281-2288.

Yazid, I.I., Mazlan, S.A., Kikuchi, T., Zamzuri, H., Imaduddin, F., (2014), “Magnetic circuit optimization in designing Magnetorheological damper”. Smart Struct Syst. **14**(5), 869-881.

Hernandez, A., Marichal, G.N., Poncela, A.V., Padron, I., (2015), “Design of intelligent control strategies using a magnetorheological damper for span structure”. Smart Struct Syst. **15**(4), 931-947.

Waitukaitis, S.R., Jaeger, H.M., (2012), “Impact-activated solidification of dense suspensions via dynamic jamming fronts”. Nature **487**(7406), 205-209.

Jiang, W.F., Gong, X.L., Xuan, S.H., Jiang, W.Q., Ye, F., Li, X.F., Liu, T.X., (2013), "Stress pulse attenuation in shear thickening fluid". Appl Phys Lett. **102**(10).

Soutrenon, M., Michaud, V., (2014), "Impact properties of shear thickening fluid impregnated foams". Smart Mater Struct. **23**(3).

Fischer, C., Braun, S.A., Bourban, P.E., Michaud, V., Plummer, C.J.G., Manson, J.A.E., (2006), "Dynamic properties of sandwich structures with integrated shear-thickening fluids". Smart Mater Struct. **15**(5), 1467-1475.

Fischer, C., Bennani, A., Michaud, V., Jacquelin, E., Manson, J.A.E., (2010), "Structural damping of model sandwich structures using tailored shear thickening fluid compositions". Smart Mater Struct. **19**(3).

Zhang, X.Z., Li, W.H., Gong, X.L., (2008), "The rheology of shear thickening fluid (STF) and the dynamic performance of an STF-filled damper". Smart Mater Struct. **17**(3).

Yeh, F.Y., Chang, K.C., Chen, T.W., Yu, C.H., (2014), "The dynamic performance of a shear thickening fluid viscous damper". J Chin Inst Eng. **37**(8), 983-994.

Ross, D., Ungar, E.E., Kerwin, E., (1959), "Damping of plate flexural vibrations by means of viscoelastic laminae". Structural damping 3, 44-87.

Kerwin Jr, E.M., (1959), "Damping of flexural waves by a constrained viscoelastic layer". J Acoust Soc Am. **31**(7), 952-962.

Zhang, X.Z., Li, W.H., Gong, X.L., (2008), "Study on magnetorheological shear thickening fluid". Smart Mater Struct. **17**(1).

Nayak, B., Dwivedy, S., Murthy, K., (2014), "Dynamic stability of a rotating sandwich beam with magnetorheological elastomer core". Eur J Me A-Solid **47**, 143-155.